Eur. Phys. J. B **19**, 345–351 (2001)

THE EUROPEAN PHYSICAL JOURNAL B

EDP Sciences

A density functional study of plutonium dioxide

X. Wu and A.K. Ray[a]

Department of Physics, University of Texas at Arlington, Arlington, TX 76019, USA

Received 16 June 2000

Abstract. The electronic and geometric structures of bulk PuO_2 and its (110) surface have been studied using a periodic model within the generalized gradient approximation (GGA) of density functional theory (DFT). The sixty core electrons of the Pu atom have been represented by a relativistic effective core potential and scalar relativistic effects have been incorporated on the valence orbitals. For bulk PuO_2, we predict an equilibrium lattice constant of 10.10 a.u. and a cohesive energy of 17.28 eV, in good agreement with experimental data. For the (110) surface, upon relaxation, the distance between the top layer and the next layer is found to decrease by 0.12 Å, *i.e.* 5.3% of the corresponding interlayer distance in the bulk. The distance between the two oxygen atoms on the top layer is found to increase by 0.15 Å, *i.e.* 5.6% of the corresponding bulk value. The small surface relaxation energy of 0.268 eV per unit cell indicates the fair stability of this surface. The effective charges on Pu and O atoms show that the chemical bonding in this system is not purely ionic. Together with the metallic feature of the density of states (DOS) on the surface, the effective charge distribution provides some basis for understanding surface reactivity and corresponding support for catalysis.

PACS. 71.15.Mb Density functional theory, local density approximation – 71.20.-b Electron density of states and band structure of crystalline solids – 73. Electronic structure and electrical properties of surfaces, interfaces, and thin films

1 Introduction

Research interest in the actinide oxides, specifically the fluorite structure light-actinide dioxides, has continued to grow over the years [1]. Among these oxides, the nature of bulk plutonium dioxide and its surface are of considerable importance from both fundamental and technological points of view [2]. In this paper, using a periodic model, we apply the techniques of modern density functional theory (DFT) to investigate the geometric and electronic structures of bulk PuO_2 and the PuO_2 (110) surface. This surface is chosen because of its reactivity with adsorbates, specifically the environmental gases and the compounds thereof. We first comment on the published results in the literature.

McNeilly [3] measured the electrical resistivity and thermoelectric power of plutonium oxide in the composition range $PuO_{1.7}$ to PuO_2 from 20 °C to 1000 °C. These measurements demonstrated that polycrystalline plutonium dioxide exhibited typical oxide semiconductor properties and the intrinsic activation energy was 1.8 eV. Veal *et al.* [4] reported systematic X-ray photoelectron spectroscopy (XPS) measurements for both core and valence electrons for oxides of several actinides, including plutonium. The XPS spectra of the localized $5f$ electrons were compared to the appropriate multiplet calculations for the neutral atom and agreement between theory and experiment was generally good. For PuO_2, the $5f$ electron spectra overlapped the weaker spectra from the O $2p$ electrons. Gubanov *et al.* [5] used the local density formalism to carry out molecular cluster calculations of the electronic structures of certain actinide monoxide and dioxides. PuO_2 was represented by a $(PuO_8)^{12-}$ cluster and non-relativistic non-self-consistent calculations were carried out in both spin-restricted and spin-polarized models, using the discrete variational method with numerical atomic basis functions. They found significant covalent mixing of the O $2p$ and Ac $5f$ atomic orbitals, making free ion crystal field models inappropriate. Courteix *et al.* [6] presented X-ray photoelectron spectra of core and valence levels for PuO_2 and Pu suboxide. The valence band spectrum of PuO_2 was compared with the results of a calculation based on a relativistically parameterized extended Huckel program, which was applied to a $(PuO_8)^{12-}$ cluster representative of the local symmetry around the Pu atom. Many features of the experimental spectrum were reproduced qualitatively from the theoretical calculations. The expected Pu $5f$-O $2p$ hybridization was also observed, as expected for the heavier actinides. Kelly and Brooks [7] applied the linear muffin-tin orbital (LMTO) method with the local density approximation (LDA) to calculate the cohesive energies, equilibrium lattice constants and bulk moduli of ThO_2, UO_2 and PuO_2. The calculated results for all three compounds

[a] e-mail: phray@research.uta.edu

agreed satisfactorily with the available experimental values. Eriksson *et al.* [8] used the film-linearized-muffin-tin-orbital (FLMTO) method to calculate the electronic structures of hydrogen and oxygen chemisorbed on plutonium. A change in the surface dipole moment was found to be induced by the chemisorbed H and O atoms and the electronic structure of the oxygen-chemisorbed state was more covalent than the hydrogen-chemisorbed state. Yamazaki and Kotani [9] used the impurity Anderson model to carry out a systematic analysis of the $4f$ core photoemission spectra of the actinide oxides AcO_2, Ac = Th–Bk. They found that PuO_2 and BkO_2 were strongly mixed valence compounds. Lander and Aeppli [10] reviewed neutron scattering studies of the magnetic properties of actinide systems. Neutron scattering experiments were able to characterize the small magnetic moments and the nature of the magnetic correlations. To study the role of the $5f$ electrons in the reactivity of actinides, Almeida *et al.* [11] studied the adsorption of O_2, CO_2, CO and C_2H_4 on Pu metal at 77 K and 296 K by UPS and XPS. For O_2, Pu_2O_3 is formed initially, followed by an oxidation to PuO_2. The results are quite different from those for the U metal. However, it was not clear that the large variety of surface reactivity was related to the gradual localization of the $5f$ electrons. The neutron inelastic-scattering experiments on PuO_2 performed by Kern *et al.* [12] disagreed with susceptibility measurements and stressed the fact that oxides are far from being understood. Using the linear combination of Gaussian-type-orbitals fitting function (LCGTO-FF) method with the LDA and the generalized gradient approximation (GGA), Boettger and Ray [13] recently studied the bulk electronic structures of PuO_2 and UO_2. The present authors recently performed a DFT study on both the bulk and surface electronic structures of PuO_2 using a set of cluster models embedded in large arrays of point charges [14]. The calculated HOMO-LUMO gap and the density of states showed the features of a typical semiconductor. The $5f$ electrons were found to be more active in chemical bonding on the (110) surface than in the bulk.

2 Computational details and results

All the computations reported in this work have been carried out on a 16-processor SGI/CRAY Origin 2000 supercomputer using the DFT package DMol^3 in the Cerius^2 program suite [15]. Numerical spin unrestricted density functional calculations are performed at the non-local GGA level [16]. Double numerical basis sets plus polarization functions (DNP) are used for both oxygen and plutonium. The sizes of these DNP basis sets are comparable to 6-31G** [17], and they are believed to be much more accurate than a Gaussian basis set of the same size [18]. A relativistic effective core potential (ECP) [19], with a small [Kr] $4d^{10}$ $4f^{14}$ core, is used for plutonium. The remaining 34 electrons (including and beyond the 5th shell) are treated as valence electrons. The scalar relativistic approach employed here was developed by Wood and Boring [20], in which a mass-velocity term and a Darwin term are added to the non-relativistic Hartree-Fock (HF) operator. However, spin-orbit splitting is not explicitly included in this approach [21].

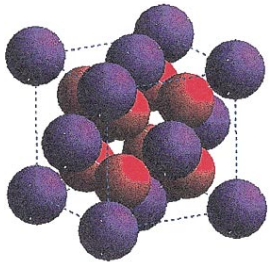

Fig. 1. Unit cell of bulk PuO_2.

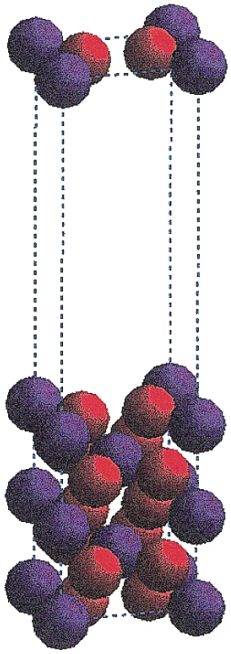

Fig. 2. Unit cell of the PuO_2 (110) surface.

For bulk computations, we first note that bulk PuO_2 has the structure of CaF_2, where plutonium forms a face centered cubic (FCC) sub-lattice inside which there is a simple cubic sub-lattice of oxygen [22]. Figure 1 illustrates the unit cell of bulk PuO_2, which contains 4 nonequivalent plutonium atoms and 8 oxygen atoms. We have used this unit cell with periodic boundary conditions to perform the necessary solid state computations for the bulk properties of PuO_2. On the other hand, the PuO_2 (110) surface has been modeled by a 5-layer slab unit cell (Fig. 2), which contains 5 nonequivalent Pu atoms and 10 oxygen atoms. The thickness of the vacuum layers has been chosen to be 15 Å, with periodic boundary conditions again. The maximum number of numerical integration mesh points available in DMol^3 has been chosen for the computations and the threshold of the density matrix convergence is set to 10^{-6}.

We first performed GGA calculations for bulk PuO_2. The specific quantities considered are the spin multiplicity, equilibrium lattice constant and cohesive energy. Initially,

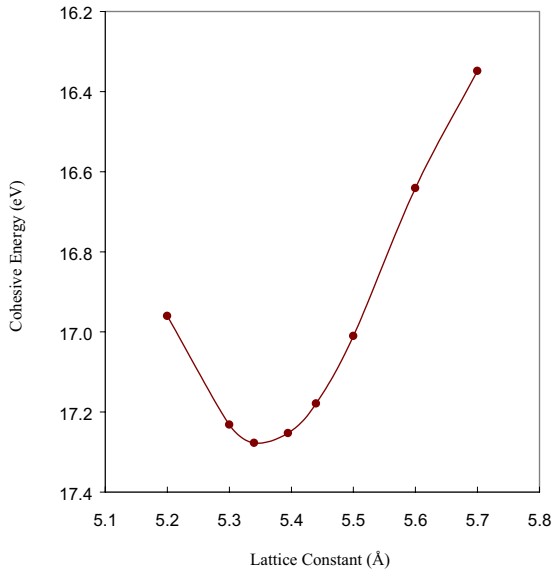

Fig. 3. Cohesive energy *vs.* lattice constant for bulk PuO_2.

the computations were done with the experimental lattice constant of $a = 5.396 \pm 0.002$ Å [22] and we studied the variation of the cohesive energy as a function of the spin multiplicity. The cohesive energy E_c is defined by:

$$E_c = (E_t(\mathrm{Pu}) + 2E_t(\mathrm{O}) - E_{tot})/n \qquad (1)$$

where $E_t(\mathrm{Pu})$ and $E_t(\mathrm{O})$ are the atomic energies for Pu and O, respectively, E_{tot} is the total energy of the unit cell, and n is the number of molecules in the unit cell. The ground state spin multiplicity of the unit cell is found to be 17 indicating the large magnetic moment in bulk PuO_2. This large spin multiplicity is mainly from the spin density of the plutonium atoms which is found to be 4.256 for each Pu atom by Mulliken charge analysis [23]. This is consistent with our previous DFT cluster calculations [14] where the unpaired $5f$ electrons were found to be the reason for the large magnetic moment. The Mulliken charge analysis also shows that charges carried by Pu and O atoms are $1.104e$ and $-0.552e$, respectively. These values of charges are much different from the ideal values for a purely ionic system, namely, $4e$ for Pu and $-2e$ for O. This indicates that PuO_2 is not a purely ionic crystal and is consistent with our previous DFT cluster computations [14] and the results of Gubanov *et al.* [5] implying that there is a covalent mixing in the chemical bonding.

We then varied the lattice constant and each possible lattice structure was spin optimized. Spin multiplicity 17 is found to be the ground state for lattice constant ranging from 5.20 Å to 5.50 Å, and 19 for 5.60 Å and 5.70 Å. This can be understood from the fact that an increase in the lattice constant values will reduce the overlapping of the charge density which, in turn, makes the spin density of Pu $5f$ electrons approach their atomic values. The cohesive energy *vs.* lattice constant is plotted in Figure 3. The equilibrium lattice constant for bulk PuO_2 is found to be 5.34 Å and the spin density of each Pu atom is 4.267.

Table 1. Comparison of available experimental and theoretical data for the equilibrium lattice constant of bulk PuO_2.

Method	Lattice constant (a.u.)
Expt. [22]	10.20
This work	10.10
LMTO [7]	10.03
LCGTO-FF (LDA-NSP) [13]	9.83
LCGTO-FF (GGA-NSP) [13]	10.03
LCGTO-FF (GGA-SP) [13]	10.12

In Table 1, we have compared our equilibrium lattice constant with other experimental and theoretical values available in the literature.

Our lattice constant is within one percent of the experimental value and is within 0.2 percent of the value obtained with the LCGTO-FF-GGA method [13]. This is to be expected since the functional used with our GGA method, namely the PW91 functional [16], is the same as used in the LCGTO-FF method. Nevertheless, this lends credibility to both calculations. As far as cohesive energy is concerned, our value of 17.28 eV is within 12.4 percent of the experimental value of 19.72 eV. Thus the cohesive energy is underestimated in our model, as also in the LMTO calculations [7]. The density of states (DOS) with the corresponding O $2p$ and the Pu $5f$ components for bulk PuO_2 with the optimized lattice constant are shown in Figure 4.

Gaussian broadening procedure has been employed here to calculate the DOS. We assigned a Gaussian $\exp(-\alpha x^2)$ to each molecular orbital eigenvalue with $\alpha = 1000$ such that the width at the half height is 0.05 eV. The DOS at each energy point comes from the contributions of all the molecular orbitals. By this broadening procedure, the band gap (or the HOMO-LUMO gap in the language of molecular orbital theory) is found to be 0.7 eV which is much smaller than our previous DFT cluster calculations of 3.21 eV [14]. Of course, a cluster is more "molecular-like" whereas these calculations are designed to simulate the bulk features. Despite the small gap, the DOS indicates that bulk PuO_2 has the general features of a semiconductor [3]. Figure 4 also shows that the valence states near the Fermi level are dominated by the Pu $5f$ states, while the valence states around -3.0 eV are mostly from the O $2p$ states together with small contribution from Pu $5f$ states. This on the other hand indicates a partial covalent nature in the chemical bonding in bulk PuO_2.

For the (110) surface, the unit cell containing 5 Pu atoms and 10 O atoms (Fig. 2) was spin-optimized at the computed equilibrium lattice constant and we only considered possible structural changes of the top layer. The primary reason behind this is that overall surface relaxation and reconstruction are expected to be rather small and might only affect the top layer. In order to see whether the two O atoms on the top layer like to move out of the plane, we relaxed the Z coordinates (normal to the surface) of the two O atoms and kept everything else frozen. It is found that the O atoms prefer to stay on the surface.

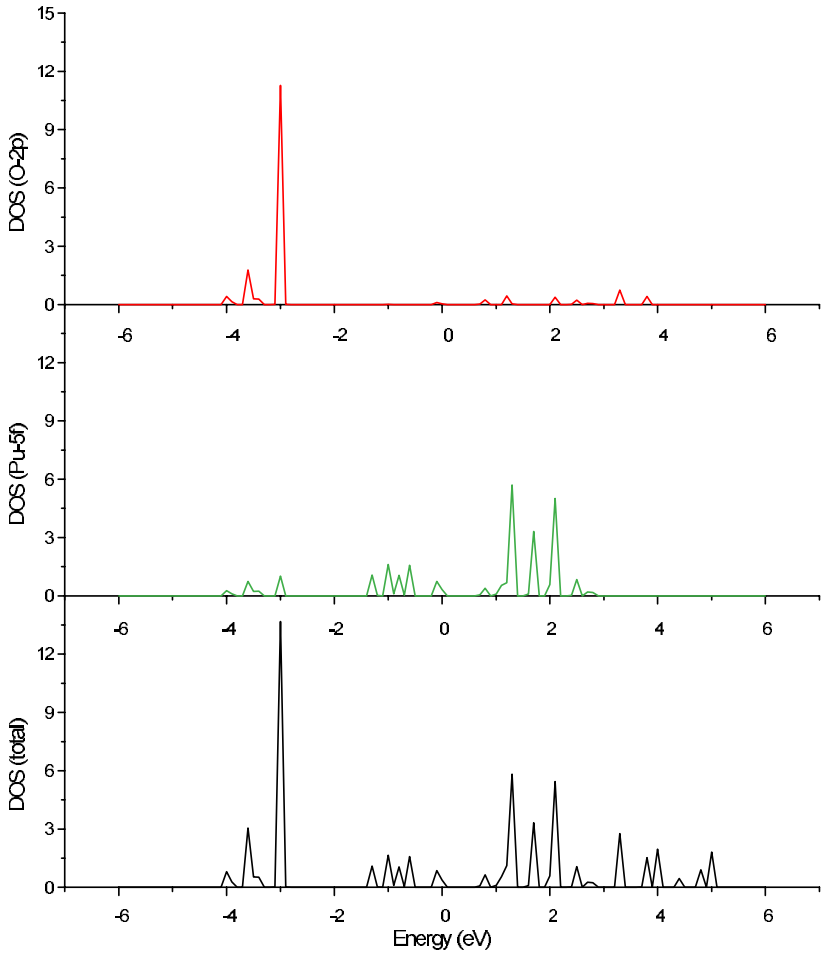

Fig. 4. The density of states (DOS) with the corresponding O $2p$ and Pu $5f$ components of bulk PuO_2 at the optimized lattice constant. The energy of the Fermi level is set to zero.

Next we relaxed the Z coordinates of all the atoms on the first layer by same amount while keeping everything else frozen at the computational bulk value. The maximum value of the cohesive energy, corresponding to the most stable position, is obtained at $\delta Z_1 = -0.12$ Å (Fig. 5). Here δZ_1 is the change in the Z-coordinate of the first layer with respect to the unrelaxed value and a negative sign implies inward relaxation. The surface relaxation energy, defined by the difference between the total energy of the unrelaxed and relaxed surfaces, is found to be 0.140 eV per unit cell. As a comparison, we note that the surface relaxation energy was computed to be 6.23 eV per unit cell for the Al_2O_3 (0001) surface by Puchin *et al.* [24]. To investigate possible reconstruction of the top layer, we optimized the distance between the two oxygen atoms, keeping all other atoms frozen. As Figure 6 demonstrates, the two O atoms prefer to increase their separation by 0.15 Å, with a surface relaxation energy of 0.143 eV comparable with the top layer relaxation.

We then relaxed these two parameters, namely, Z_1 (the Z coordinates of the first layer atoms) and d_{oo} (distance between the two O atoms on the top layer) simultaneously.

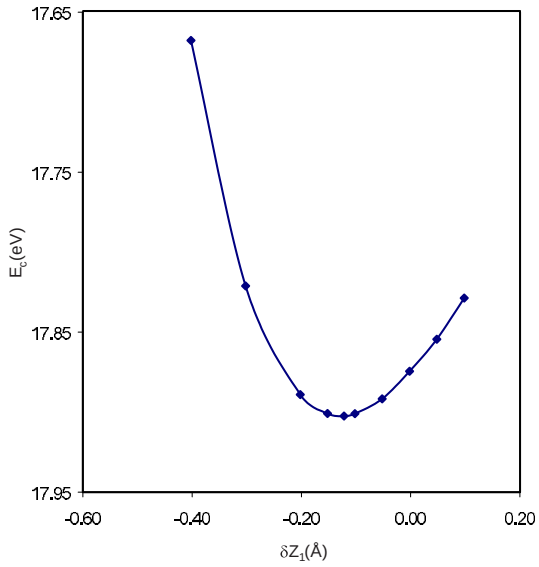

Fig. 5. Cohesive energy E_c *vs.* δZ_1, where δZ_1 is the change of the Z coordinates of the first layer atoms with respect to the unrelaxed value. The positive value means outward relaxation.

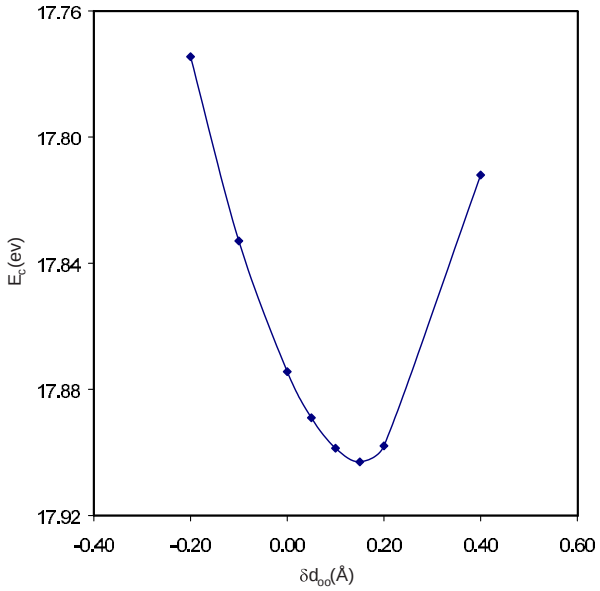

Fig. 6. Cohesive energy E_c *vs.* δd_{oo}, where δd_{oo} is the change in distance between the two oxygen atoms on the top layer with respect to the optimized bulk value of 2.67 Å.

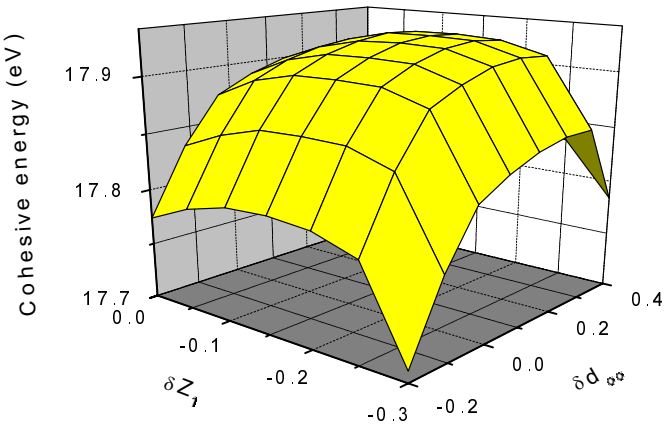

Fig. 7. Cohesive energy surface as a function of δZ_1(Å) and δd_{oo}(Å). δZ_1 is the change in the Z coordinates of the top layer atoms with respect to the unrelaxed value. δd_{oo} is the change in distance between the two oxygen atoms with respect to the corresponding bulk value.

The cohesive energy surface as a function of δZ_1 and δd_{oo}(a positive value of the change of d_{oo} implies a preferred increase in separation) is plotted in Figure 7. The optimized value for δZ_1 and δd_{oo} are -0.12 Å and 0.15 Å, respectively, *i.e.*, the top layer moves inwards by 0.12 Å with the two O atoms being pushed further away by 0.15 Å. The surface relaxation energy is again found to be rather small, namely 0.268 eV per unit cell, indicating that the PuO_2 (110) surface is pretty stable.

We also performed Mulliken analysis [23] to compute the spin density of the Pu atoms and the effective charges carried by the Pu and O atoms for both ideal and relaxed (110) surfaces. The results are summarized in Table 2. Unlike the bulk where each Pu atom has the same spin density of 4.267, the spin densities are different for Pu atoms on different layers for the surface. It can be seen that the Pu atoms on the surface layers (both the top and the fifth layers) carried larger spin density than those of the sandwiched layers, which show that the magnetic moment is larger on the surface than in the bulk. This can be reasoned by the symmetry broken on the surface, which reduces the coordination number of the surface atoms and hence reduces the overlapping of the charge density and makes the magnetic moment of plutonium approach its atomic value. The charges carried by Pu and O atoms show that the chemical bonding is not ideally ionic. On different layers, the charges carried by Pu and O atoms are different. Each layer is ionic, with the surface layers (the first and the fifth layers) being negatively charged and the three bulk layers positively charged though the whole unit cell is neutral. The electrical field generated by the charged surface layers might be partly responsible for the chemical reactivity and the support for catalysis on the surface. However, we also notice the observable difference in the Pu spin density and the effective charges carried by Pu and O atoms between the middle layer of the surface slab and the bulk. For example, the spin density of the Pu atom for the bulk is 4.267 to be compared with a spin density of 4.039 for the middle layer. Also, the effective charges carried by Pu and O atoms for the bulk are $1.104e$ and $-0.552e$, respectively, whereas the corresponding effective charges for the middle layer of the (110) surface are $1.569e$ and $-0.617e$. This indicates that a thicker slab may be needed to give more accurate description of the surface properties. The DOS and the corresponding O $2p$ and Pu $5f$ components of the PuO_2 (110) surface with the top layer relaxed and reconstructed are plotted in Figure 8.

The same type of broadening procedure as mentioned before was used here. We note here a mixture of the O $2p$ and Pu $5f$ states in both valence and conduction bands. Unlike the bulk DOS, which showed the semiconductor features, the surface DOS showed more metallic features, which is due to the surface states originated from the broken symmetry. This might also explain the surface reactivity.

In summary, non-local GGA computations have been carried out for the geometric and electronic structures of bulk PuO_2 and its (110) surface. For bulk PuO_2, the equilibrium lattice constant and the cohesive energy are found to be in good agreement with available experimental and theoretical data. The DOS of bulk PuO_2 shows the semiconductor features though the band gap is fairly small. The surface relaxation and reconstruction of the PuO_2 (110) surface have been investigated for the top layer using a periodic slab model. The energetically favorable geometry of the top layer is found to be displaced inwards by 0.12 Å with the distance between the two oxygen atoms increased by 0.15 Å. However, the low surface relaxation energy indicates that the ideal (110) surface of

Table 2. Mulliken analysis for the spin densities of the Pu atoms and the charges carried by the Pu and O atoms on different layers of both unrelaxed and relaxed PuO_2 (110) surfaces.

	Unrelaxed			Relaxed and reconstructed		
Layer	Spin density	Effective	charges	Spin density	Effective	charges
No.	Pu	Pu	O	Pu	Pu	O
1	4.406	0.776	−0.570	4.276	0.736	−0.578
2	3.964	1.404	−0.602	3.978	1.468	−0.600
3	3.997	1.557	−0.614	4.039	1.569	−0.617
4	3.964	1.404	−0.602	4.011	1.389	−0.605
5	4.406	0.776	−0.570	4.447	0.775	−0.570

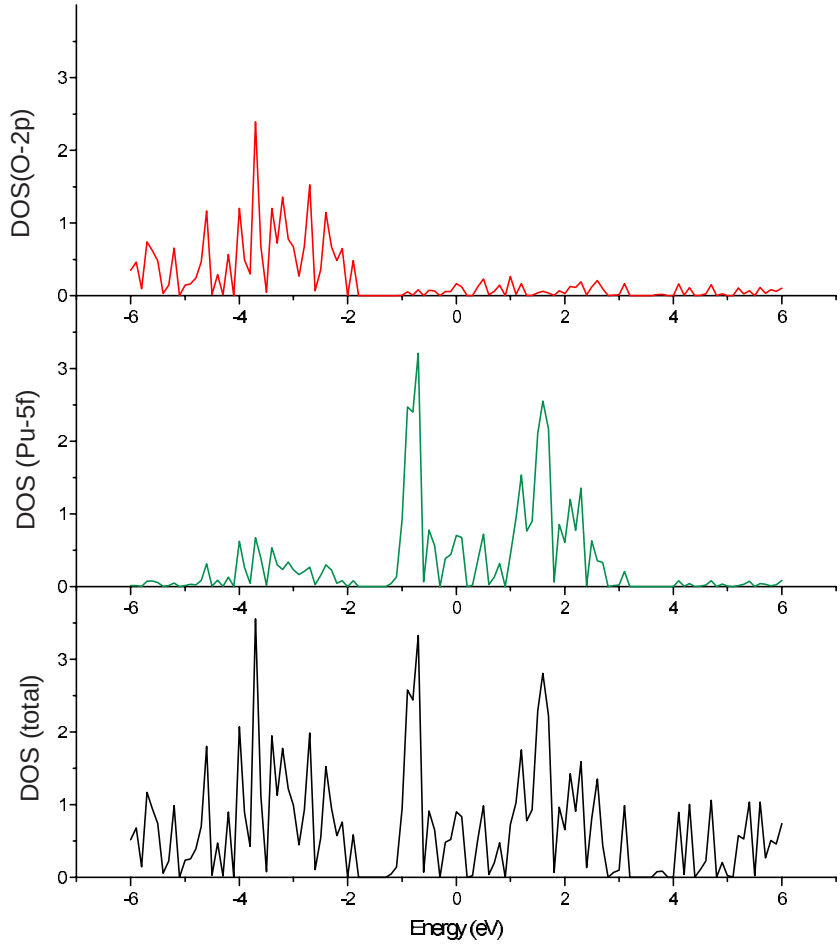

Fig. 8. Density of states with the corresponding O $2p$ and Pu $5f$ components of PuO_2 (110) surface with the top layer relaxed and reconstructed. The energy of the HOMO is set to zero.

PuO_2 is rather stable. The larger spin density of Pu atoms on the surface layers agreed with the general belief that the broken symmetry on the surface might enhance magnetism [25]. The non-neutrality of the surface layers and the metallic DOS feature might, in part, be the reason for surface reactivity and the corresponding support for catalysis.

This manuscript is prepared with the support of the U.S. Department of Energy (DOE), Cooperative Agreement No. DE-FC04-95AL85832. However, any opinions, findings, conclusions, or recommendations expressed herein are those of the authors and do not necessarily reflect the views of DOE. This work was conducted through the Amarillo National Research Center.

References

1. *Plutonium Futures - The Science, AIP Conference Proceedings 532*, edited by K.K.S. Pillay, K.C. Kim (2000).
2. J.M. Haschke, T.E. Ricketts, J. Alloys Compd. **252**, 148 (1997).
3. C.E. McNeilly, J. Nucl. Mat. **11**, 53 (1964).
4. B.W. Veal, D.J. Lam, H. Diamond, H.R. Hoekstra, Phys. Rev. B **15**, 2929 (1977).
5. V.A. Gubanov, A. Rosen, D.E. Ellis, J. Phys. Chem. Solids **40**, 17 (1978).
6. D. Courteix, J. Chayrouse, L. Heintz, R. Baptist, Sol. St. Comm. **39**, 209 (1981).
7. P.J. Kelly, M.S.S. Brooks, J. Chem. Soc. Faraday Trans. **83**, 1189 (1987).
8. O. Eriksson, Y.G. Hao, B.R. Cooper, G.W. Fernando, L.E. Cox, J.W. Ward, A.M. Boring, Phys. Rev. B **43**, 4590 (1991).
9. T. Yamazaki, A. Kotani, J. Phys. Soc. Jpn **60**, 49 (1991).
10. G.H. Lander, G. Aeppli, J. Magn. Magn. Mater. **100**, 151 (1991).
11. T. Almeida, L.E. Cox, J.W. Ward, J.R. Naegele, Surf. Sci. **287/288**, 141 (1993).
12. S. Kern, R.A. Robinson, H. Nakotte, G.H. Lander, B. Cort, P. Watson, F.A. Vigil, Phys. Rev. B **59**, 104 (1999).
13. J.C. Boettger, A.K. Ray, *23rd Annual Actinide Separations Conference Abstracts, Pasco, Washington, 1999; ibid. 1999 Researchers' Conference Abstracts, Amarillo National Resource Center, Amarillo, Texas*; *ibid.* Int. J. Quant. Chem. (in press); reference [1], *ibid.* p. 422.
14. X. Wu, A.K. Ray, Physica B (to be published).
15. B. Delley, J. Chem. Phys. **92**, 508 (1990); A. Kessi, B. Delley, Int. J. Quant. Chem. **68**, 135 (1998); B. Delley, Int. J. Quant. Chem. **69**, 423 (1998).
16. J.P. Perdew, Y. Wang, Phys. Rev. B **46**, 12947 (1992).
17. W.J. Hehre, L. Radom, P.V.R. Schleyer, J.A. Pople, *Ab Initio Molecular Orbital Theory* (John Wiley and Sons, New York, 1986).
18. *DMol*^{3} - *Cerius*^{2}*/Quantum Chemistry, Release 3.8*, (MSI, San Diego, 1998).
19. W. Kuchle, M. Dolg, H. Stoll, H. Preuss, J. Chem. Phys. **100**, 7535 (1994).
20. J.H. Wood, A.M. Boring, Phys. Rev. B **18**, 2701 (1978).
21. E.F. Archibong, A.K. Ray, J. Mol. Struct. **530**, 165 (2000); N. Ismail, J.-L. Heully, T. Saue, J.-P. Daudey, C.J. Marsden, Chem. Phys. Lett. **300**, 296 (1999).
22. I. Narai-Szabo, *Inorganic Crystal Chemistry* (Academia Kiado, Budapest, 1969); U. Benedict, G.D. Andreetti, J.M. Fournier, A. Waintal, J. Phys. Lett. France **43**, L171 (1982); U. Benedict, W.B. Holzapfel, *Handbook on the Physics and Chemistry of Rare Earths* **17**, 245 (1993); N.V. Dedov, V.F. Bagryantsev, Radiochemistry **38**, 24, (1996).
23. R.S. Mulliken, J. Chem. Phys. **23**, 1833, 1841, 2338, 2343 (1955).
24. V.E. Puchin, J.D. Gale, A.L. Shluger, E.A. Kotomin, J. Gunster, M. Brause, V. Kempter, Surf. Sci. **370**, 190 (1997).
25. D.L. Mills, Phys. Rev. B **3**, 3887 (1971); *ibid.* **8**, 4424 (1973).